Journal of Applied Polymer Science

Effect of the Crosslinking Density and Programming Temperature on the Shape Fixity and Shape Recovery in Epoxy–Anhydride Shape-Memory Polymers

Xue Lian Wu,[1] Shu Feng Kang,[2] Xiao Jing Xu,[1] Feng Xiao,[1] Xiao Lan Ge[1]

[1]School of Mechanical Engineering, Jiangsu University, 301 Xuefu Road, Zhenjiang 212013, People's Republic of China
[2]Shenzhen Woer Heat-Shrinkable Material Company, Limited, Lanjing Road, Shenzhen 518118, People's Republic of China
Correspondence to: X. L. Wu (E-mail: xlwu@ujs.edu.cn)

ABSTRACT: In addition to the fabrication of thermoset epoxy–anhydride shape-memory polymers (SMPs), a systematic experimental investigation was conducted to characterize the crosslinking density, micromorphology, thermal properties, mechanical properties, and shape-memory effects in the epoxy SMP system, with a focus on the influence of the crosslinking density and programming temperature on the shape-fixity and shape-recovery behaviors of the polymers. On the basis of the crosslinking density information determined by NMR technology, we concluded that the effect of the crosslinking density on the shape-fixity behaviors was dependent on the programming temperature. The advantage of a nice combination of crosslinking density and programming temperature provided an effective approach to tailor the actual shape recovery within a wide range. The increasing crosslinking density significantly improved the shape-recovery ratio, which could be further improved through a decrease in the programming, whereas the crosslinking density was more fundamental. This exploration should play an important role in the fabrication and applications of SMP materials. © 2014 Wiley Periodicals, Inc. J. Appl. Polym. Sci. **2014**, *131*, 40559.

KEYWORDS: crosslinking; property relations; stimuli-sensitive polymers; structure

Received 29 July 2013; accepted 3 February 2014
DOI: 10.1002/app.40559

INTRODUCTION

As a promising actively moving polymer, shape-memory polymers (SMPs) have drawn increasing attention in smart materials fields in recent years.[1–4] The most unique characteristic of SMPs is their capability of recovering their original shape in response to an external stimulus after deformation and fixation in a temporary shape. Temperature variation is one of the most common stimuli for actuating SMPs,[5,6] and other stimuli have been achieved by the application of light,[7] electrical energy,[8–12] magnetic fields,[13,14] or solutions.[15–19] SMPs can find broad applications in deployable space structures,[20] biological equipments,[21] textile materials,[22] and micrometer-sized actuators.[23] In recent days, alongside with continuous efforts to develop new applications of SMPs, proposed novel applications, such as temperature labels and anticounterfeit labels, have emerged.[24–26]

From a real engineering application point of view, the optimization shape-memory effect (SME) in polymers has turned out to be a major concern in many engineering fields. According to previous studies, the SME in polymers can be tailored by chemical and physical methods, that is, the designation of a chemical structure (with a focus on the chemistry group or crosslinking density), the adjustment of the programming parameters (temperature or strain), changes in the actuating parameters (heating temperature or time),[27–32] and so on. Working mechanisms on optimization of the SME in polymers have also been explored.[33] However, the study of the extent of optimization of the SME, particularly on the tailored shape-fixity ratio (R_f) and shape-recovery ratio (R_r), is still underdeveloped.

The measurement of crosslinking density is one of the most efficient methods for revealing structural information on a crosslinked polymer network, in which *netpoints* are the nodes of macromolecule segments attributed to physical coiling or chemical connectivity. In a thermally responsive SMP that uses a glass transition to achieve the SME, the flexibility is a function of the temperature, as it can be softened or hardened upon heating or cooling to realize a large deformation, shape fixity, and shape recovery. Crosslinking netpoints always remain hard during the shape-memory cycle, and this actuates the flexible segments to recover to their original state after deformation. The relative motion of segments and netpoints determined by the crosslinking density are the primary mechanism of the SME in polymers;[34,35] this can be explained by the dual-state mechanism according to ref. 5, in which the molecular chain was considered

© 2014 Wiley Periodicals, Inc.

Table I. Composition of the Epoxy SMPs

Sample	DMP 421 (g)	Anhydride hardener (g)	Accelerator (g)	DGEG (g)
SMP1	100	80	0.16	14.4
SMP2	100	80	0.16	21.6
SMP3	100	80	0.16	28.8
SMP4	100	80	0.16	36.0
SMP5	100	80	0.16	45.0

the rubber phase, and the netpoint is considered the glassy phase. Alicia et al.[27] investigated how free- and fixed-strain SMEs of (meth)acrylate-based SMPs could be tuned independently through their crosslinking density and long-term storage. Initial studies have demonstrated how the glass-transition temperature (T_g) and thermal and thermomechanical properties were tailored by the crosslinking density in the epoxy SMP system.[36,37] However, the relationship between the crosslinking density and SME has yet to be fully studied.

On the other hand, in previous studies, the most common traditional methods used to investigate crosslinking density of polymers are equilibrium swelling and mechanical measurement;[38–40] these methods are not capable for providing complete reliable information on chemically crosslinked polymer networks.[41] One of the most informative and sensitive methods is solid-state NMR relaxation experimentation, in which the crosslinking density is directly measured by the analysis of the molecular chain length between netpoints with respect to the chain mobility.[42,43] The sensitivity of the NMR relaxation parameters to local molecular motions makes this technique unique for the investigation of the molecular dynamic changes in the physical structure or mobility of the network.[41]

Recent investigations proved that the programming temperature does have a strong influence on the shape fixity and recovery progress upon heating.[5,44,46] A study on epoxy SMPs found that the maximum recovery rate was achieved at about the previous programming temperature.[44] Another study revealed that an increase in the programming temperature led to an increase in the R_f value in a commercial biodegradable polymer, DPEF9910, whereas it resulted in a decrease in R_r by theoretical analysis.[5]

According to its unique thermomechanical properties together with its excellent SME, thermoset epoxy SMPs have greater potential applications in the field of functional and structural materials.[4] For example, most structural-grade composite components for spacecraft applications incorporate epoxy SMPs rather than other polymers because of the better mechanical performance, ease of fabrication, and environmental durability inherent in epoxy SMPs.[20] Relatively little work has been done on anhydride-cured epoxy polymer systems dealing with shape-memory behaviors, which are less prone to absorb moisture and more easily moldable compared with amine and carboxylic acid cured epoxy SMPs.[36,47–50]

In this study, an anhydride-cured epoxy SMP system was fabricated. Its thermal stability, glass transition, mechanical properties, and microtopography were first studied. Then, the effect of the crosslinking density, which was quantitatively determined by the NMR technique, and the programming temperature on the SME in the epoxy SMPs were investigated.

EXPERIMENTAL

Materials

A thermosetting epoxy-based SMP was fabricated by an epoxy resin, anhydride hardener, accelerator, and toughening reagent. The anhydride hardener (*cis*-4-methyl-1,2,3,6-tetrahydrophthalic anhydride, purchased from Qingyang Chemical Co., Ltd., Jiaxing, China) and accelerator (ethylene glycol, BASF Chemical Co., Ltd., analytical reagent) were mixed by an electric blender at room temperature (20°C) for 30min. Then, liquid epoxy resin (DMP421, weight per epoxy equivalent = 128–140, Shanghai Zhengxingfa Co.) and a toughening reagent [diglycidyl ethers of ethylene glycol (DGEGs) number-average molecular weight = 281, supplied by Sigma-Aldrich] were added to the mixture and stirred electrically at 20°C for 2 h. All materials for the polymer synthesis were used as received. The weight ratio of the epoxy resin and hardener was 1:0.8, and the accelerator was used at a concentration of 0.2% of the hardener weight. Different amounts of the DGEG monomer (8, 12, 16, 20, and 25 wt % of the total comonomer solution, respectively) were used, and different levels of crosslinking of the copolymer were obtained by this DGEG monomer. The compositions of the epoxy SMPs are shown in Table I. After it was degassed in a vacuum furnace (to remove bubbles), the comonomer mixture was injected into a plate mold composed of two glass slides separated by a silica gel rod spacer. Polymerization was accomplished by a heating curing process, which was performed at 135°C for 4 h. All of the samples were cut from the bulk sheet with a laser cutter for testing. It should also be noted that the DGEG monomer and anhydride hardener were different with the composition used in ref. 37.

Characterization

NMR. ^{13}C-NMR measurements were carried out with an MR-CDS 3500 crosslinking density spectrometer at a magnetic field strength of 0.35 Tesla; this corresponded to a 15-MHz proton resonance frequency. The used cylindrical sample was 3 mm in diameter and 8 mm in height.

Thermogravimetric Analysis (TGA). TGA test (TGA 2950, Surplus Solutions, Inc.) was conducted from 25 to 500°C with a ramp rate of 10°C/min.

Differential Scanning Calorimetry (DSC). The thermal properties of the polymers were characterized with a DSC-Netzsch 204 (Germany). The samples were heated from −40 to 200°C,

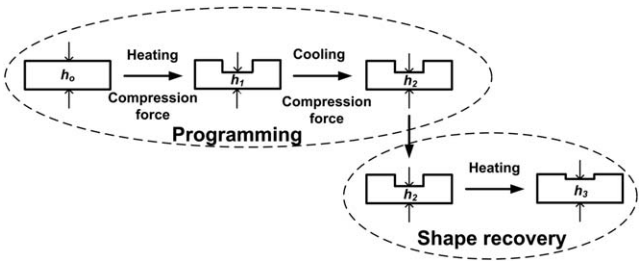

Figure 1. Illustration of a typical SME cycle in a heating-responsive SMP with uniaxial compression programming.

cooled down to −40°C, and then heated again to 200°C. Heating and cooling rates of 10°C/min were used for the detection of the glass transitions.

Dynamic Mechanical Analysis (DMA). DMA testing was performed on a DMA Q800 (Netzsch DMA 242) in a tension mold from −40 to 200°C at a rate of 5°C/min with a constant frequency of 5 Hz with rectangular samples with dimensions of 30 × 5 × 1 mm^3.

Tensile Testing. An isothermal quasi-static tension test was carried out on a Zwick/Roell Z010 (Zwick GmbH, Ulm, Germany) equipped with a long travel extensometer at room temperature (25°C), and samples for the tension test were laser-cut from the polymer sheet into standard samples (ASTM D 638, type IV) and strained at an elongation rate of 1 mm/min.

Scanning Electron Microscopy (SEM). SEM (Camscan, MX2600) was used to observe the fracture surface morphology of the polymers. Specimens for SEM were prepared from the cross sections of the fractured samples after tensile testing.

SME. Samples for shape-memory behavior testing were cut by a laser from the thin polymer sheets as a square strip (ca. 30 × 30 × 4 mm^3), referred to as the permanent shape. A series of compression tests were conducted to program each epoxy polymer with same original thickness ($h_0 = 4$ mm) by an Instron 5565 instrument, which had a temperature-controllable chamber for heating. A constant strain rate of 0.1%/s was applied in both loading and unloading in all of the compression tests.

A typical thermoresponsive SME cycle in the epoxy SMPs included two processes, as illustrated in Figure 1.

The sample was heated inside the temperature-controllable chamber for 20 min at a prescribed temperature [e.g., glass-transition start (T_{gs}), T_g, and glass-transition finish (T_{gf}), which were measured with a thermocouple attached to the tested sample] and was then compressed with a metal mandrel by an Instron 5565 for cylinder identification (10 mm in diameter, 2 mm in depth). Subsequently, the sample was cooled (to $T_{gs} - 30$°C) and unloaded, and a residual depth upon unloading for the identification was obtained. All of the compression tests were uniaxial to ensure the same programmed compression strain for each sample. The depth of the identification was measured five times by a thickness gauge, whose accuracy reached 0.001 mm. This was the programming process.

Subsequent shape-recovery tests were carried out according to the exact programming conditions. The sample was gradually heated in a furnace to their respective $T_{gs} - 20$°C, $T_{gs} - 10$°C, T_{gs}, T_g, and T_{gf} for 30 min, and then, they were cooled to $T_{gs} - 30$°C for 20 min. After cooling, the final residual thickness of the compressed part in the sample (h_3) after shape recovery was measured again.

Correspondingly, R_f and R_r are normally defined by the following equations:

$$R_f = \frac{h_0 - h_2}{h_0 - h_1} \quad (1)$$

$$R_r = \frac{(h_0 - h_2) - (h_0 - h_3)}{h_0 - h_2} = \frac{h_3 - h_2}{h_0 - h_2} \quad (2)$$

As illustrated in Figure 1, h_1 and h_2 denote the minimum thickness upon loading and the residual thickness upon unloading, respectively. Correspondingly, $h_0 - h_1$, $h_0 - h_2$, and $h_0 - h_3$ are the maximum programming depth, residual depth upon unloading, and final residual depth after heating for the identification in the sample, respectively. Note that for simplicity, the change in the diameter of the cylinder identification was neglected in the SME cycle, and the value of the maximum compression strain was the same (50%), as h_0 was 4 mm and $h_0 - h_1$ was 2 mm for each sample.

In this study, the investigation of R_r was conducted at the same temperature value relative to the T_g of the respective polymer; this assured that all networks were in an equivalent state of macromolecular motion. Subsequently, this was more convenient for providing a normalized comparison for the study of the effect of crosslinking density on the shape fixity and shape recovery of the epoxy SMPs. We assumed that the time-dependent parameters and thermal strain were negligible, as the viscoelastic effect and thermal expansion were negligible because of the applied small constant strain rate (0.1%/s) and temperature variation (<60°C), respectively, in this study.

RESULTS AND DISCUSSION

Crosslinking Density

The crosslinking density is a crucial factor for most properties of crosslinked networks and shows great influence on their physical and mechanical properties.[38] The crosslinking density can be quantitatively identified by the spatially resolved determination of the NMR transverse relaxation time (T_2),[41] as T_2 is the preferred relaxation parameter as a probe for a crosslinked polymer network structure. Figure 2 presents the T_2 values of the epoxy SMPs (SMP1, SMP2, SMP3, SMP4, and SMP5). As shown in Figure 2, the T_2 value of the five epoxy SMPs increased from 0.15 to 0.36 ms; this was a more accurate experimental result compared to those found with traditional methods[38–40] and supplied reliable information on the crosslinking density. T_2 revealed the chain length between crosslinking points and then its corresponding mobility. A higher T_2 value indicated that the chain segments were loosely restricted by netpoints and favored a higher mobility; this reflected a lower crosslinking density.[42,43] Therefore, as the T_2 value increased, the crosslinking density decreased for the five epoxy SMPs with increasing DGEG monomer content.

In a thermoset crosslinked polymer network, the motion of segments was significantly affected by the distribution of netpoints,

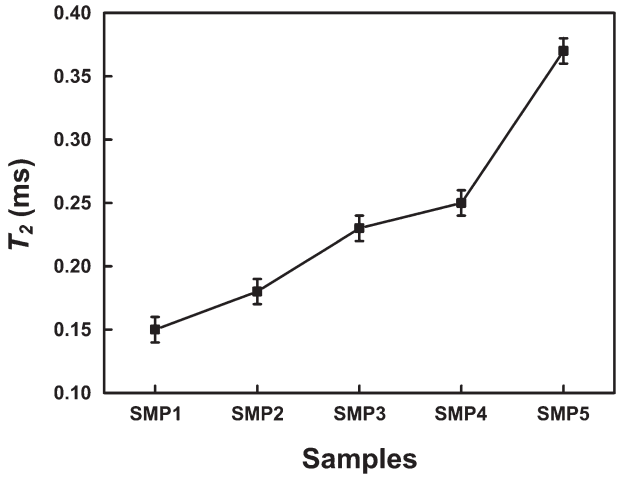

Figure 2. T_2 values of the five epoxy SMPs obtained from NMR testing.

and the relaxation time for the polymer materials could be largely governed by constraints on a large spatial-scale chain mobility imposed by the chemical crosslinks. Thus, T_2 relaxation is very sensitive even to small differences in the crosslinking density. In this study, the decreasing crosslinking density was attributed to the increasing DGEG monomer content; this resulted in the far distance between netpoints in the network.

Thermal Properties

Figure 3 presents the TGA curves of the five epoxy SMPs with decreasing crosslinking density. According to Figure 3, there was virtually almost no weight loss before 300°C; this confirmed the similarity in the high thermal stability of the polymer system. The similar decomposition temperatures for the epoxy SMPs revealed that the variation in the crosslinking density had no influence on the thermal stability; this was determined by the bond-dissociation energy (due to the types of chemical bonds) in the polymer network.

T_g is a key important parameter for the shape fixity and shape recovery of SMP materials; this is usually determined by a DSC test. With a heating/cooling rate of 10°C/min, the T_g and corresponding breadth of glass transition ($T_{gf} - T_{gs}$) for the epoxy

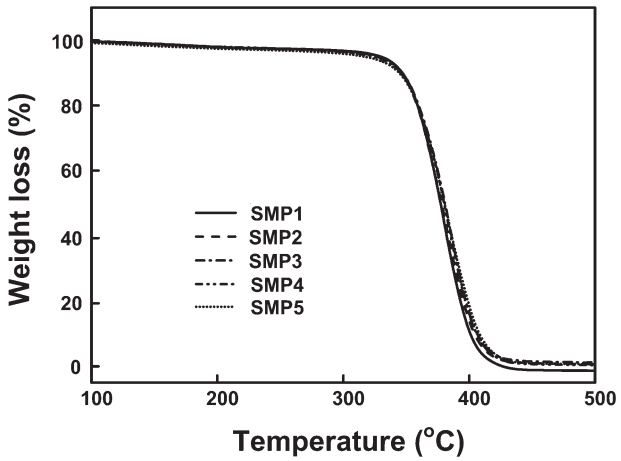

Figure 3. TGA curves of the epoxy SMPs with decreasing crosslinking density.

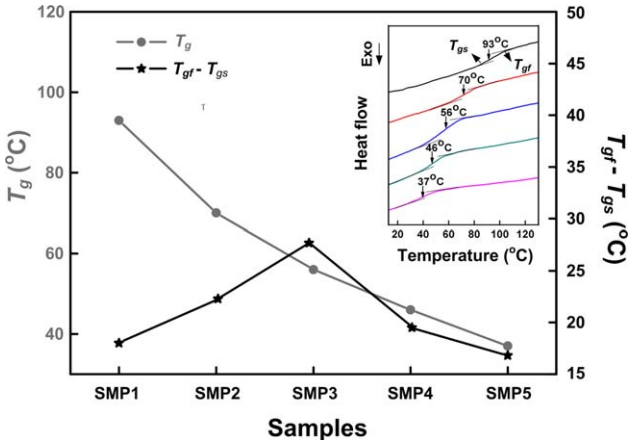

Figure 4. Values of the T_g and breadth of the glass transition ($T_{gf} - T_{gs}$) of the epoxy SMPs with decreasing crosslinking density. The black line represents $T_{gf} - T_{gs}$, and the gray line represents T_g. The inset shows a zoomed-in view of the DSC curves. [Color figure can be viewed in the online issue, which is available at wileyonlinelibrary.com.]

polymers with decreasing crosslinking density are presented in Figure 4.

As shown in Figure 4, there was no crystalline transition but only one glass transition for each polymer according to DSC curves. This revealed that the different chemical compositions were compatible in the network and that the polymers were amorphous.

According to Figure 4, T_g decreased with decreasing crosslinking density between 93 and 37°C; this was an ideal example of how the thermal properties (T_g) of a copolymer system could be altered through the control of the crosslinking density. In an amorphous thermoset polymer network, the polymer chains take up a completely random distribution and are prevented from slipping from each other by crosslinking points. In this study, with decreasing crosslinking density, netpoints are linked farther with longer flexible chains and a lower degree of steric hindrance; this leads to a higher chain mobility and then results in a decrease in T_g. This study revealed different trends for T_g versus the crosslinking density versus those found in previous work.[36]

Figure 4 also shows that the breadth of the glass transition increased and then decreased with a peak value at SMP3 according to decreasing crosslinking density. As the glass transition reveals the essential transition from freezing to the free motion states of segments, the breadth of glass transition depends on the inhomogeneity in the segment length between netpoints; that is, the greater the segment length inhomogeneity was, the larger was the breadth of glass transition. Therefore, we deduced that the segment length inhomogeneity between netpoints increased and then decreased. This was attributed to increasing longer segments between the three-dimensional crosslinked polymer networks. This was important for revealing information on changes in the crosslinked chemical structure of the polymers.

DMA

The unique mechanical properties of polymer materials include viscoelasticity, which exhibits both elastic and viscous

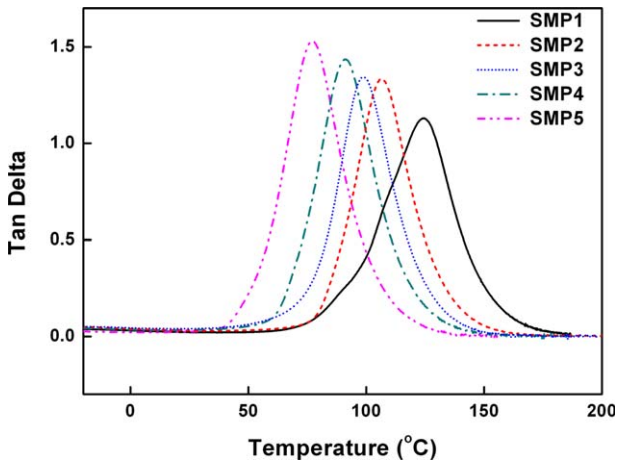

Figure 5. Tanδ versus temperature for the epoxy SMPs with decreasing crosslinking density. [Color figure can be viewed in the online issue, which is available at wileyonlinelibrary.com.]

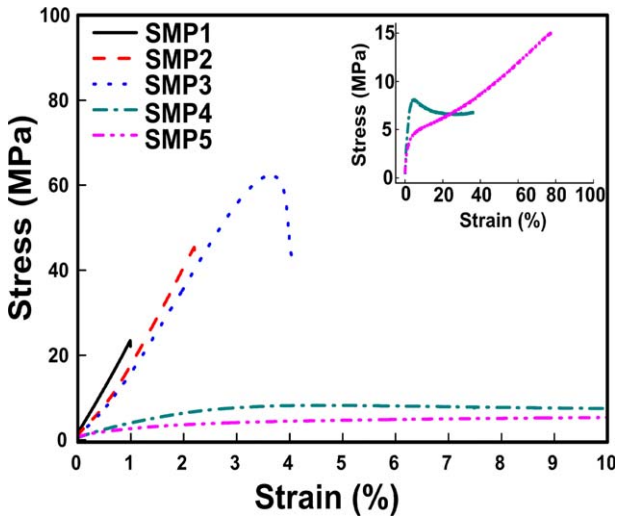

Figure 6. Representative stress–strain curves of the epoxy SMPs with decreasing crosslinking density at room temperature. [Color figure can be viewed in the online issue, which is available at wileyonlinelibrary.com.]

characteristics during deformation. Tanδ corresponds to the ratio of the loss modulus to the storage modulus, which is usually used to evaluate the damping properties of polymer materials. The effect of the crosslinking density on the damping properties was examined in this study. Figure 5 reveals the tan δ of the polymers with decreasing crosslinking density in the temperature range from −20 to 200°C. According to Figure 5, there was only one tanδ peak for each sample, and this confirmed the compatible composition in the epoxy SMP system, which was revealed by the DSC result. As shown in Figure 5, the peak value of tanδ increased from 1 to 1.5 with decreasing crosslinking density, and the corresponding peak temperatures were about 131, 102, 90, 84, and 63°C at a heating rate of 5°C/min with a constant frequency of 5 Hz. These values were slightly higher than the T_g's obtained from the DSC results. A larger tanδ implies that the polymer is more likely viscous than elastic. Therefore, the decreasing crosslinking density enhanced the viscous properties of the polymers and then the damping properties. This was attributed to the longer and increasingly flexible properties of the molecular chains between netpoints. A higher viscosity prevent the polymer from undergoing brittle failure, and this deduction was confirmed by the results of the tensile tests, as discussed next.

Tensile Testing

Five tensile samples were used for each epoxy polymer, and the representative stress–strain curves are shown in Figure 6. In particular, the stress–strain behavior of the polymers transitioned gradually from a pronounced brittle response to a high elastic response as the crosslinking density decreased. To obtain a better view of the effect of the crosslinking density on the tensile mechanical properties, the strength, elongation at break (ε_B), and elastic modulus of the polymers are summarized in Figure 7.

Figure 7(a) shows the dependence of the strength on the crosslinking density at room temperature (25°C). It is clear that the strength increased and then decreased with decreasing crosslinking density and showed a peak value for SMP3. For instant, the tensile strength of SMP1 was 15 MPa. This increased three times for SMP2 and four times for SMP3; then, it decreased sharply with a further decrease in the crosslinking density and showed values below 10 MPa for SMP4 and SMP5. Netpoints were mainly responsible for carrying the load, as they prevent the flexible segments from slipping from each other.[34] Because a

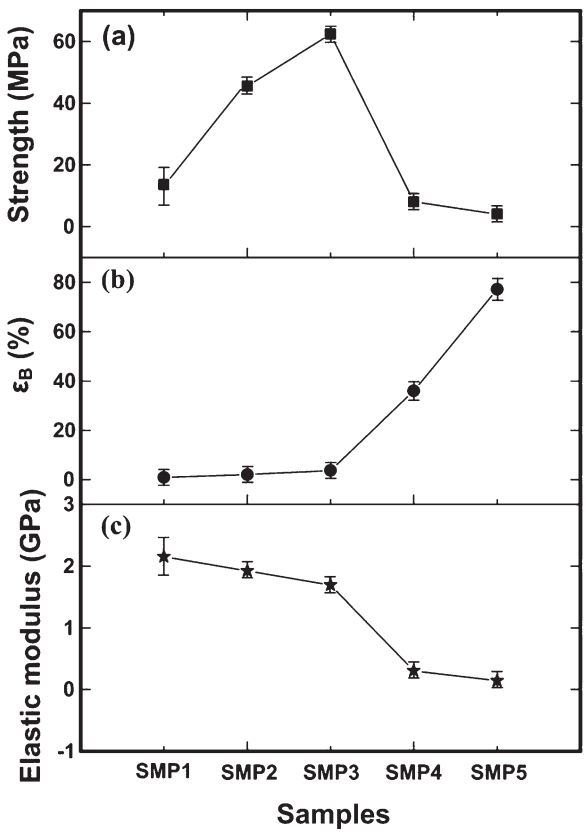

Figure 7. Strength, ε_B, and elastic modulus of the epoxy SMPs with decreasing crosslinking density at room temperature.

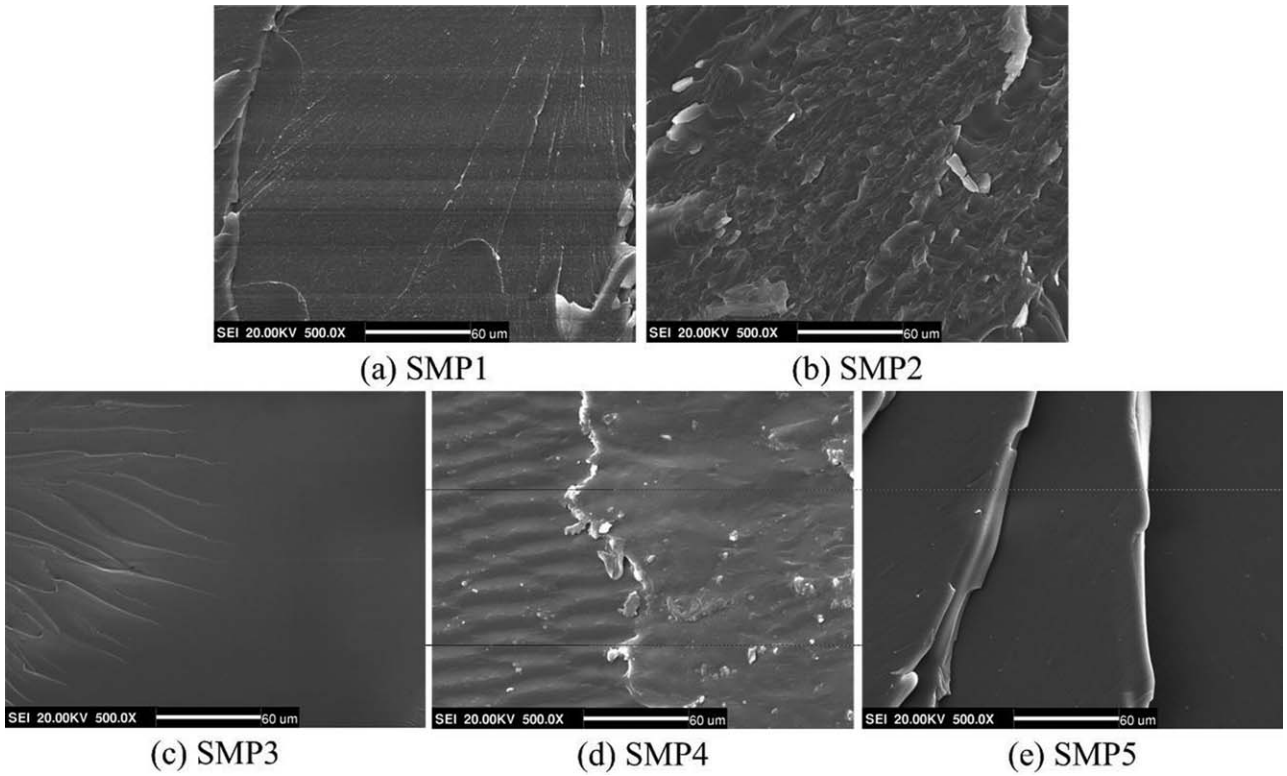

Figure 8. SEM images of the tensile fracture surface of the epoxy SMPs with decreasing crosslinking density.

decreasing crosslinking density means a decreasing number of netpoints in the polymer network, a decrease in the tensile strength was expected. However, in this study, the tensile strength increased with decreasing crosslinking density from SMP1 to SMP3, and this was possibly due to the excessively higher crosslinking density of these networks. This led to higher brittle properties, limited the capability of the carrying load, and resulted in a lower tensile strength. The same trend in the tensile strength with decreasing crosslinking density was found in other polymers.[35]

Figure 7(b) represents the influence of the crosslinking density on the polymer stretchability (ε_B). ε_B increased slightly (between 0.96 and 3.8%) with decreasing crosslinking density from SMP1 to SMP3. After that, ε_B started to increase dramatically from SMP3 to SMP5 and was between 36 and 77.2%. Figure 7(c) plots the elastic modulus of the polymers with decreasing crosslinking density. Obviously, the elastic modulus decreased with decreasing crosslinking density.

We concluded that the crosslinking density calculated from T_2 was the primary reason for the variety of macroscopic mechanical properties of the crosslinked epoxy SMPs. The decreasing crosslinking density resulted in an increasing distance between netpoints, and then, the package action of the netpoints on the segments was weakened. Therefore, as the crosslinking density decreased, the segments with an inherently high flexibility were linked loosely together with a lower steric hindrance effect, and this resulted in a decrease in the elastic modulus and an increase in ε_B. ε_B revealed the toughness properties and was the limiting factor in the deformation capability of the polymers. Of particular attention was the fact that the decreasing crosslinking density (from SMP1 to SMP3) increased the toughness without a sacrifice in the strength of the polymers. This was a significant improvement compared with prior work.[29]

SEM

Figure 8 presents the SEM images of the fracture surfaces of the polymers with decreasing crosslinking density. Figure 8(a) is the fracture surface of SMP1, which had the highest crosslinking density among the five polymers. The figure shows that there was much more crack with sharp edges along the same direction in the smooth fracture surface; this indicated a typical brittle crack. As shown in Figure 8(b), the sharp crack trended downward, and the crack direction spread around; this showed a toughness trend. Although another dispersing phase appeared, as shown in Figure 8(c), this tended to be more obvious with decreasing crosslinking density, as shown in Figure 8(d,e).[43] The changing trend of the fracture surface from brittle crack to toughness crack was a sign of the greater extent of microphase separation in the networks with decreasing crosslinking density. The second microphase forbade the crack extension by absorbing crack energy, and this resulted in an increase in toughness. The possible reason for the decrease in the crosslinking density was that the second flexible phase entered the network of the polymer. Therefore, the toughness of the polymers was increased by the dispersion of stress and the increase in the crack energy of the system with decreasing crosslinking density. The results of SEM were in good agreement with that obtained from tensile testing. In addition, the microphase separation did

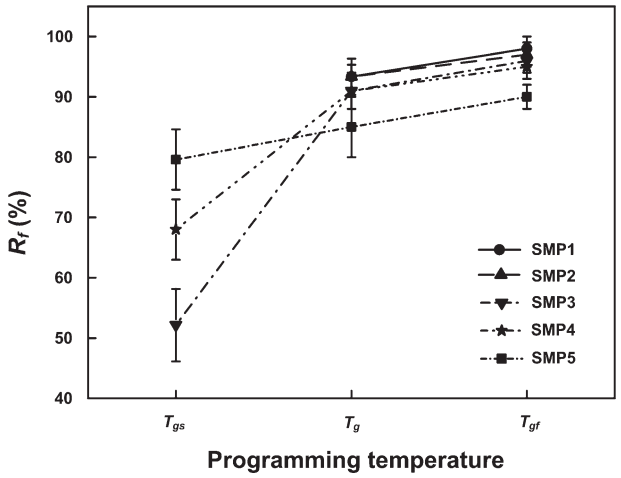

Figure 9. R_f versus programming temperature for the epoxy SMPs with decreasing crosslinking density with uniaxial compression programming.

not affect the compatible properties of the components in the polymer according to the DSC results.

SME

Figure 9 presents the relationship of R_f versus the programming temperature for the epoxy SMPs with decreasing crosslinking density. As shown in the figures, a higher programming temperature resulted in a higher R_f for each polymer; this was more obvious for the SMP with a higher crosslinking density, particularly around the lower half of the T_g range. For instant, the actual R_f increased from about 51% at T_{gs} to about 90% at T_g and then 93% at T_{gf} for SMP3, whereas for SMP5, the R_f values were 78, 83, and 86% at T_{gs}, T_g, and T_{gf}, respectively.

Figure 9 reveals that the effect of the crosslinking density on the shape-fixity behaviors depended on the programming temperature. For example, R_f increased at T_{gs} and decreased at T_g and T_{gf} with decreasing crosslinking density. The epoxy SMPs with higher crosslinking densities (SMP1 and SMP2) could not be programmed at T_{gs} because of the higher brittleness.

On the basis of previous experimental results, an R_f of about 50% or more was always achievable when the programming temperature was within the glass transition for a maximum programming strain of 50% for the epoxy SMP system.

It was reasonable to conclude that both the crosslinking density and programming temperature could effectively influence R_f for the epoxy SMP system; this was due to the different viscoelastic characteristics of the SMPs with various crosslinking densities and different programming temperatures.[51] When programmed at T_{gs}, each polymer showed more glassy behavior and higher elasticity; this resulted in a lower R_f, particularly for polymers with higher crosslinking densities. The mobility of the polymer chain significantly improved at T_g and even improved further (the chains were relatively easy to flow) at T_{gf}, and much more plastic deformation took place for the certain maximum programming strain (50%). Thus, R_f increased with increasing programming temperature; this was same as the trend listed in refs. 5 and 52.

The higher the crosslinking density is, the shorter the average segment is between netpoints in the polymer network. Programming for the polymer with higher crosslinking density should require a larger stretching deformation in segments to reach the same maximum strain in the material. Therefore, an increase in the crosslinking density resulted in a higher R_f because of the resulting higher residual strain at the respective T_g and T_{gf}.

Figure 10 presents the R_r as a function of the heating temperature from $T_{gs} - 20°C$ to $T_{gf} + 10°C$ for each epoxy SMP with decreasing crosslinking density and programming at T_g, T_{gf}, and $T_{gf} + 10°C$. The crosslinking density decreased for the epoxy SMPs (SMP1, SMP2, SMP3, SMP4, and SMP5) according to the NMR results in Figure 2.

According to Figure 10, it was clear that a higher heating temperature led to a higher R_r until full shape recovery was reached at or above T_g. More importantly, Figure 10 also revealed that a higher crosslinking density resulted in a higher R_r; this was more true when the sample was heated at T_{gs}, whereas this trend weakened at T_g and vanished gradually as the activation temperature increased up to T_{gf}. For instance, at a heating temperature of T_{gs} with different programming temperatures, R_r was above 90% for SMP1 and SMP2, whereas it ranged from 60 to 80% for SMP3 and SMP4 and was between 30 and 60% for SMP5.

According to the previous experimental results, in any case, an R_r of about 90% or more was accomplished upon heating to T_g for the polymers (except R_r was from 70 to 90% for SMP5). It should be reasonable to conclude that the shape-recovery ability of this epoxy SMPs was excellent. The previous results also highlight the significant capacity to readily adjust the shape-recovery behaviors according to the crosslinking density; this was beneficial to SMP materials.

Full shape recovery may not be a must in all engineering applications, as long as the amount of recovery can meet the requirements of a specific application. Therefore, particular attention should be paid on the lowest actuation temperature (relative to T_g) for significant shape recovery. As shown in Figure 10, the lowest actuation temperature increased according to decreasing crosslinking density. For instance, although the recovery ratio was always less than 20% and even near zero for a lower crosslinking density when the sample was heated at $T_{gs} - 20°C$ for each polymer, a large R_r (>50%) with different programming temperatures was realized when the sample was heated at $T_{gs} - 10°C$ for SMP1 and SMP2, at T_{gs} for SMP3 and SMP4, and at T_g for SMP5. Significant shape recovery occurred even at temperatures much lower than the glass transition for SMP1 and SMP2; this was different from results of previous studies.[21,36,37]

Because a larger deformation in chains is essential for polymers with a higher crosslinking density for certain programming strains at the same relative temperature, a higher elastic strain energy stored in the polymer provides a higher driving force for subsequent thermally induced shape recovery. Thus, in the case of the same applied programming strain (50%) in this epoxy SMP system, the stored internal energy barrier between the

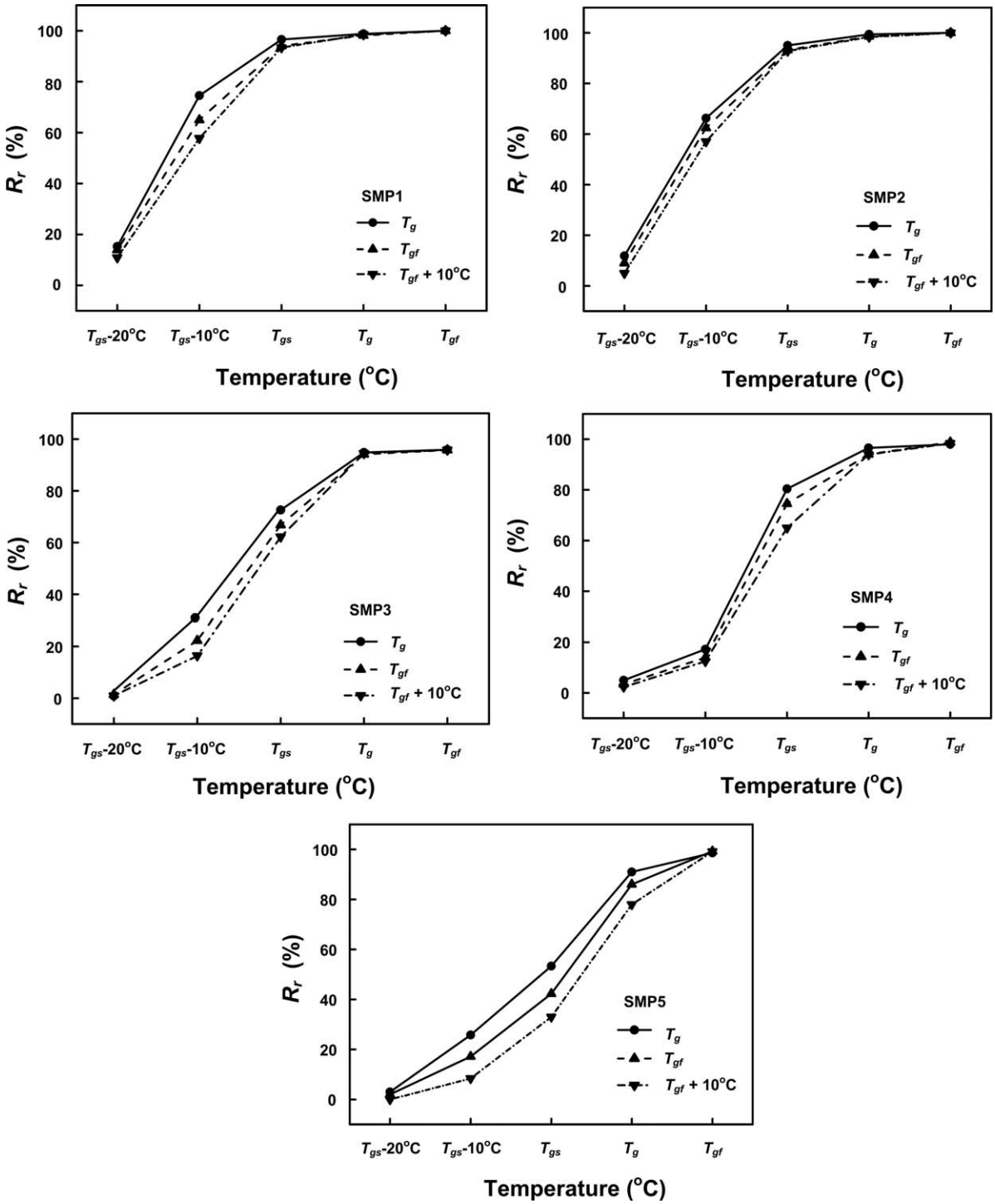

Figure 10. R_r as functions of the heating temperature ($T_{gs}-20°C$, $T_{gs}-10°C$, T_{gs}, T_g, T_{gf}) and programming temperature (T_g, T_{gf}, and $T_{gf}+10°C$) for the epoxy SMPs with decreasing crosslinking density.

original shape and programmed shape is crosslinking density dependent, that is, high at a high crosslinking density and low at a low crosslinking density. Therefore, samples with a higher crosslinking density showed a higher recovery ratio when they were heated at the same temperature relative to T_g. Full recovery was reached for each SMP at T_{gf}, as the segment (transition component) was able to flow easily but was incompressible.

According to Figure 10, the exact level of R_r was also dependent on the programming temperature, that is, a higher programming temperature resulted in a lower R_r at the same relative heating temperature, particularly for polymers with lower crosslinking density. The underlying reason behind this phenomenon was the significant amount of plastic deformation in the netpoints and/or nonreversible flow in the segments with

increasing programming temperature. Programming conducted at or above the glass transition prevented permanent plastic deformation and provided a higher shape fixity (to minimize the elastic recovery upon unloading in programming), whereas a lower programming temperature resulted in an increase in the shape recovery, although a higher programming force was needed. Therefore, the selection of the programming temperature is essential for optimization in SME and dependent on detailed engineering applications.

As the purpose of this study was the optimization of the SME in polymers, we focused on R_f and R_r tailored by a chemical method (changes in the crosslinking density) and physical method (the adjustment of the programming temperature). According to previous experiment results, both the crosslinking density and programming temperature could significantly adjust R_f and R_r, respectively, to obtain higher R_f and R_r values with a lower energy consumption. However, as the programming temperature and heating temperature were determined by T_g; this was dependent on the crosslinking density. The crosslinking density was key and was more effective for optimizing SME in the epoxy SMP system compared with the programming temperature and heating temperature. In addition, properties such as T_g, breadth of glass transition, damping properties, strength, flexible properties, and elastic modulus were also adjusted by the crosslinking density; this was attributed to the mobility of restricted segments between netpoints. The adjustable properties were essentially important from the view of real engineering, as SMPs often were used under some complicated environmental factors, such as for biomedical applications or aerospace applications.

CONCLUSIONS

In this study, a systematic investigation was conducted to study the thermoresponsive SME in a fabricated thermoset epoxy–anhydride SMP system with various crosslinking densities at different programming temperatures under the stress state of uniaxial compression.

The main conclusions are as follows.

- An excellent SME was observed in the epoxy–anhydride SMPs with different crosslinking densities and programming temperatures. R_f was above 50%, and R_r ranged from 75 to 99% when the sample was heated at T_g in almost all of the experiments.
- Both R_f and R_r were dependent on the crosslinking density and programming temperature. Increasing the crosslinking density decreased R_f ($R_f \leq 80\%$) when the programming temperature was below T_g and increases R_f ($R_f \geq 80\%$) with a programming temperature at or above T_g. R_r increased with increasing crosslinking density when the samples were heated at T_{gs} or T_g. On the other hand, the lower programming temperature decreased R_f, and increased R_r. Through careful selection of the crosslinking density and programming temperature, the SME could be optimized. For instance, a higher crosslinking density and lower programming temperature resulted in a higher R_r.
- In comparison with the programming temperature, the crosslinking density was more important for the optimization of SME in the polymer materials. The adjustment of the programming temperature is a physical method for tailoring the SME in polymers, whereas the crosslinking density optimizes the SME by designation of the chemical structure in polymers and is a chemical method.

ACKNOWLEDGMENTS

This project was partially supported by the National Natural Science Foundation of China (contract grant number 51303070).

REFERENCES

1. Lendlein, A. Shape-Memory Polymers; Springer: Berlin, **2010**.
2. Huang, W. M.; Ding, Z.; Wang, C. C.; Wei, J.; Zhao, Y.; Purnawali, H. *Mater. Today* **2010**, *13*, 54.
3. Xie, T. *Nature* **2010**, *464*, 267.
4. Santhosh Kumar, K. S.; Biju, R.; Reghunadhan, Nair, C. P. *React. Funct. Polym.* **2013**, *73*, 421.
5. Huang, W. M.; Zhao, Y.; Wang, C. C.; Ding, Z.; Purnawali, H.; Tang, C.; Zhang, J. L. *J. Polym. Res.* **2012**, *19*, 9952.
6. Wang, C. C.; Huang, W. M.; Ding, Z.; Zhao, Y.; Purnawali, H. *Compos. Sci. Technol.* **2012**, *72*, 1178.
7. Lendlein, A.; Jiang, H. Y.; Junger, O.; Langer, R. *Nature* **2005**, *434*, 879.
8. Lu, H. B.; Liang, F.; Gou, J. H. *Soft Matter* **2011**, *7*, 7416.
9. Lu, H. B.; Gou, J. H. *Polym. Adv. Technol.* **2011**, *23*, 1529.
10. Lu, H. B.; Gou, J. H. *Nanosci. Nanotechnol. Lett.* **2012**, *4*, 1155.
11. Lu, H. B.; Huang, W. M. *Appl. Phys. Lett.* **2013**, *102*, 231910.
12. Lu, H. B.; Bai, P. P.; Yin, W. L.; Liang, F. *Nanosci. Nanotechnol. Lett.* **2013**, *5*, 732.
13. Buckley, P. R.; McKinley, G. H.; Wilson, T. S.; Small, W.; Benett, W. J.; Bearinger, J. P.; McElfresh, M. W.; Maitland, D. *J. IEEE Trans. Biomed. Eng.* **2006**, *53*, 2075.
14. Yu, K.; Westbrook, K. K.; Kao, P. H. *J. Compos. Mater.* **2013**, *47*, 51.
15. Huang, W. M.; Yang, B.; Fu, Y. Q. Polyurethane Shape Memory Polymers; CRC: Boca Raton, FL, **2013**.
16. Huang, W. M.; Yang, B.; Li, A.; Li, C.; Chan, Y. S. *Appl. Phys. Lett.* **2005**, *86*, 114105.
17. Lu, H. B. *J. Appl. Polym. Sci.* **2013**, *127*, 2896.
18. Lu, H. B. *J. Appl. Polym. Sci.* **2012**, *123*, 1137.
19. Lu, H. B.; Huang, W. M. *Pigment Resin Technol.* **2013**, *42*, 237.
20. Gall, K.; Mikulas, M.; Munshi, N. A.; Beavers, F.; Tupper, M. *J Intell. Mater. Syst. Struct.* **2000**, *11*, 877.
21. Lendlein, A.; Langer, R. *Science* **2002**, *296*, 1673.
22. Chen, S. J.; Hu, J. L.; Liu, Y. Q.; Liem, H. M.; Zhu, Y.; Meng, Q. H. *Polym. Int.* **2007**, *56*, 1128.
23. Mitsuhiro, E.; Koichiro, U.; Naokazu, I.; John, M. H.; Takao, A. *Soft Matter* **2013**, *9*, 3074.

24. Huang, W. M.; Wu, X. L. (to Tianlang Pharmaceutical Co., Ltd.). Chin. Pat. 201210480325.5 (**2012**).
25. Huang, W. M.; Wu, X. L. (to Tianlang Pharmaceutical Co., Ltd.). Chin. Pat. 201310045236.2 (**2013**).
26. Xie, T.; Xiao, X. C.; Li, J. J.; Wang, R. M. *Adv. Mater.* **2010**, *22*, 4390.
27. Ortega, A. M.; Yakacki, C. M.; Dixon, S. A.; Likos, R.; Greenberg, A. R.; Gall, K. *Soft Matter* **2012**, *8*, 7381.
28. Feldkamp, D. M.; Rousseau, I. A. *Mater. Eng.* **2010**, *295*, 726.
29. Safranski, D. L.; Gall, K. *Polymer* **2008**, *49*, 4446.
30. Revathi, A.; Rao, S.; Rao, K. V.; Singh, M. M.; Murugan, M. S.; Srihari, S.; Dayananda, G. N. *J. Polym. Res.* **2013**, *20*, 113.
31. Yakacki, C. M.; Shandas, R.; Safranski, D.; Ortega, A. M.; Sassaman, K.; Gall, K. *Adv. Funct. Mater.* **2008**, *18*, 2428.
32. Leonardi. A. B.; Fasce, L. A.; Zucchi, I. A.; Hoppe, C. E.; Soulé, E. R.; Pérez, C. J.; Williams, R. J. *J. Eur. Polym. J.* **2011**, *47*, 362.
33. Sun, L.; Huang, W. M.; Wang, C. C.; Zhao, Y.; Ding, Z.; Purnawali, H. *J. Polym. Sci. Part A: Polym. Chem.* **2011**, *49*, 3574.
34. Lendlein, A.; Kelch, S. *Angew. Chem. Int. Ed.* **2002**, *41*, 2034.
35. Kim, B. K.; Lee, S. Y. *Polymer* **1996**, *37*, 5781.
36. Xie, T.; Rousseau, I. A. *Polymer* **2009**, *49*, 4446.
37. Leng, J. S.; Wu, X. L.; Liu, Y. *J. Smart Mater. Struct.* **2009**, *18*, 095031.
38. Nelson, B. A.; Kinga, W. P.; Gall, K. *Appl. Phys. Lett.* **2005**, *86*, 103108.
39. Safranskia, D. L.; Gall, K. *Polymer* **2008**, *49*, 4446.
40. Flory, P. *J. Polym. J.* **1985**, *17*, 1.
41. Litvinov, V. M.; Dias, A. A. *Macromolecules* **2001**, *34*, 4051.
42. Orza, R. A.; Magusin, P. C. M. M.; Litvinov, V. M.; Duin, M. V.; Michels, M. A. J. *Macromolecules* **2007**, *40*, 8999.
43. Adriaensens, P.; Storme, L.; Carleer, R.; Dhae, J.; Gelan, J.; Litvinov, V. M.; Marissen, R.; Crevecoeur, J. *Macromolecules* **2007**, *35*, 135.
44. Xie, T.; Page, K. A.; Eastman, S. A. *Adv. Funct. Mater.* **2011**, *21*, 2057.
45. Xie, T. *Polymer* **2011**, *52*, 4985.
46. Kratz, K.; Madbouly, S. A.; Wagermaier, W.; Lendlein, A. *Adv. Mater.* **2011**, *23*, 4058.
47. Zhang, C. H.; Wei, H. G.; Liu, Y. Y.; Tan, H. F.; Guo. Z. H. *High Perform. Polym.* **2012**, *24*, 702.
48. Biju, R.; Reghunadhan, Nair, C. P. *J. Polym. Res.* **2013**, *20*, 82.
49. Rousseau, I. A.; Xie, T. *J. Mater. Chem.* **2010**, *20*, 3431.
50. Fan, M. J.; Yu, H.; Li, X. G.; Cheng, J.; Zhang, J. Y. *Smart Mater. Struct.* **2013**, *22*, 055034.
51. Wu, X. L.; Zheng, H.; Liu, Y. J.; Leng, J. S. *Int. J. Mod. Phys. B* **2010**, *24*, 2386.
52. Wu, X. L.; Huang, W. M.; Tan, H. X. *J. Polym. Res.* **2013**, *20*,150.